Carpathian Journal of Earth and Environmental Sciences, August 2019, Vol. 14, No. 2, p. 353 - 366; DOI:10.26471/cjees/2019/014/086

APPLICATION OF REMOTE SENSING AND GIS TO WATER TRANSPARENCY ESTIMATION IN RESERVOIRS

Joanna JASKUŁA[1] & Mariusz SOJKA[1]

[1]Institute of Land Improvement, Environmental Development and Geodesy, Poznań University of Life Sciences, Piątkowska 94, 60-649 Poznań, Poland, e-mail: jaskula@up.poznan.pl; masojka@up.poznan.pl

Abstract: The paper presents the use of satellite imagery, GIS applications and in-situ measurements for the estimation of water transparency in reservoirs. Satellite data from the Sentinel-2 sensor and interpolation methods (Kriging, IDW, Natural Neighbour, Spline, Trend) were used for Secchi Disk Transparency (SDT). The results of this study show that the Sentinel-2 blue/red band ratio is a reliable predictor of SDT with the coefficient of determination equal to 0.83 ($p < 0.001$). The analysis indicates low coefficients of determination between the SDT calculated using interpolation methods based on GIS and in-situ measurements. The SDT modelled on the basis of satellite imagery was further used to indicate parts of the reservoir characterized by the highest uncertainty. The high uncertainty occurs near the shoreline of the reservoir and near the dam, which might be related to spectral reflectance from wooded areas, the overgrowth process or small depth of water. Additionally, it was observed that the highest uncertainty associated with the applied individual regression occurs in the case of limit values of the B2/B4 ratio which were not used during regression model development. The results show that more than 91% of the reservoir is characterized by a standard deviation less than 0.2, while only 0.25% shows values higher than 0.5. The results indicate that the application of remote sensing has important significance for water transparency estimation in reservoirs.

Keywords: reservoir, water transparency, Secchi disk, satellite imagery, Sentinel-2

1. INTRODUCTION

Lakes, reservoirs and ponds are among the most important components of the Earth's natural resources, especially as they provide the largest volume of surface freshwater for human use (Kim et al., 2019; Pekel et al., 2016; Zhang et al., 2017). Due to various factors connected with human activity (Dąbrowska et al., 2016; Bogdał et al., 2015; Borek, 2018), reservoir parameters (Dąbrowska et al., 2018) and climate changes (Soundharajan et al., 2016; Yan et al., 2018), inland waters are increasingly exposed to changes in water quality, including water clarity and eutrophication. The aquatic environment is characterized by high temporal and spatial variability (Policht-Latawiec et al., 2014), especially due to the high impact of climate parameters (air temperature, precipitation). According to Dąbrowska et al., (2016), spatial variability of water quality parameters also depends on anthropogenic pressures such as agricultural activities or waste-water management in the catchment. Due to the large number of factors influencing inland water parameters, it is necessary to find an interpolation method which will take into account the local variation of water quality.

One of the most frequently used parameters to assess water quality is water transparency, measured on the basis of the Secchi disk (Lee et al., 2015; Philippart et al., 2013). Secchi disk transparency (SDT) is defined as a depth when a white and black disk with a diameter equal to 0.3 m is no longer visible to an observer. Measurements of SDT have been used in many studies (Fleming-Lehtinen & Laamanen, 2012; Nishijima et al., 2016; Zhou et al., 2018) to determine the eutrophic state and ecological status. Traditional monitoring of water quality parameters is determined by in-situ measurements and laboratory analyses (Bus & Mosiej, 2018; Sender et al., 2018; Xu et al., 2017). Collecting samples from the field ensures high accuracy of the data in single locations. Unfortunately, analyzing numerous samples from the field is a time-consuming and expensive process

(Cavalli et al., 2009; Hestir et al., 2015). Moreover, in-situ measurements provide information limited only to point-based representation and do not give a spatial overview of water bodies (Odermatt et al., 2012; Zhengjun et al., 2008).

In the past few decades, with development of GIS applications, computer techniques became the most powerful tools for mapping spatial and temporal changes in the environment. In-situ measurements are used for applying interpolation methods, which create continuous surfaces on the basis of discrete points (Bhunia et al., 2016; Gong et al., 2014; Liang et al., 2018; Shen et al., 2019). Interpolation methods allow values to be predicted for the whole area where the measurement has not been taken. The most commonly used interpolation techniques are Kriging, Inverse Distance Weighting (IDW), Natural Neighbour, Spline and Trend methods (ESRI, 2012). However, there is no single reference interpolation method that produces the most reliable results.

Nowadays, remote sensing offers the most valuable opportunities in Earth monitoring, especially due to the unique advantage of effective and reliable mapping of the environment from space (Chawira et al., 2013; Dlamini et al., 2016; Dörnhöfer et al., 2018b; Jaskuła et al., 2018; Majozi et al., 2014; Martins et al., 2018). Since the last decade, free satellite imagery (Landsat, MERIS, MODIS, Sentinel missions) has increasingly changed the possibilities of water monitoring. Long-term collection of high-quality data is necessary to understand, better manage and mitigate the impact of climate changes on the environment and civil safety (Aschbacher & Milagro-Pérez, 2012; Dörnhöfer et al., 2018a; Laurent et al., 2014). Satellite imagery is used for natural hazards, and agricultural and aquatic applications, mainly because of its multi-spectral characteristics (Agutu et al., 2017). Additionally, spatial and time resolution of satellites makes it possible to observe areas of interest more precisely. Remote sensing data have been used in numerous studies to analyze the state of the aquatic environment (including water transparency and eutrophication) and additionally are used to build relationship with in-situ measurements. These relationships enable one to predict values at uncontrolled points (Giardino et al., 2001; Hicks et al., 2013; Li et al., 2017; Shi et al., 2015). Most of the studies have focused on the relationship between Landsat imagery and in-situ measurements (Giardino et al., 2001; Hicks et al., 2013; Li et al., 2017; McCullough et al., 2012; Ren et al., 2018; Rodriguez et al., 2014; Sass et al., 2007). Since 2015 one of the most promising sources of data seems to have been the Sentinel mission, which is part of the Copernicus Earth Observation mission, previously known as Global Monitoring for Environment and Security (GMES). The GMES programme was developed for monitoring and dissemination of environmental and security information. The mission is financed by the European Union and managed by the European Space Agency (ESA). The main purpose of the Sentinel missions is to provide European policy makers, researchers and the public with up-to-date and accurate information about the state of the environment (Donlon et al., 2012).

The primary objective of this study was to formulate and validate a practical method to estimate Secchi disk depth by combination of satellite and in-situ measurements. The second purpose was to compare the capabilities of interpolation methods based on GIS applications and Sentinel-2 imagery for determining water transparency in reservoirs. Additionally, the authors attempted to determine the uncertainty of the selected interpolation method in different parts of the reservoir. The study assumes the following research hypothesis: satellite imagery allows more accurate assessment of the spatial variability of Secchi disk transparency than classical interpolation methods based on GIS.

2. MATERIALS AND METHODS

2.1. Study site

Jezioro Kowalskie reservoir (52°28′39.781″ N, 17°9′49.022″ E) is located in the centre of the Warta basin, the third biggest river in Poland (Fig. 1). The surface area of the reservoir is 203 ha and the total capacity 6.58 mln m^3. Jezioro Kowalskie is a source of water for agricultural purposes, but also performs other functions, including flood reduction, maintenance of minimum acceptable flows and recreation (Sojka et al., 2016). The reservoir has a two-stage construction, being split into two parts – the main and pre-dam reservoir, separated by an additional dam. The main reservoir has the same functions as an ordinary single-part reservoir – it stores water for many purposes. The study area in this paper is mainly focused on the pre-reservoir, which plays a specific role. The pre-reservoir is the smaller part and it is used to store sediments and limits the inflow of pollutants to the main part. The area of the pre-dam reservoir in Jezioro Kowalskie is 40.4 ha and its capacity is 0.590 m m^3. The mean depth of this part is 1.3 m while that of the main reservoir is 3.68 m (Hydroprojekt, 2004).

Due to the population and urbanization development in the last decades, the Jezioro Kowalskie catchment has suffered from intensive anthropogenic and agricultural pressure. According to the Regional Inspectorate of Environmental Protection in Poznań, the physicochemical state of the Główna river, which

inflows to Jezioro Kowalskie, was evaluated to below the 'good' class (Regional Inspectorate of Environmental Protection, 2016). It was mainly caused by high values of nitrogen and phosphorus compounds, whose concentrations vary from 7.5 to 28 mg $N \cdot dm^{-3}$ with a mean of 17.2 mg $N \cdot dm^{-3}$ for total nitrogen and from 0.144 to 3.43 mg $P \cdot dm^{-3}$ with a mean of 1.607 mg $P \cdot dm^{-3}$ for total phosphorus. According to Sojka et al., (2017) these values significantly exceed permissible and dangerous levels determined for Jezioro Kowalskie on the basis of the Vollenweider model (1976) and could lead to eutrophication and a decrease of water transparency, especially in the pre-dam zone which is characterized by a small depth and rapid increase of water temperature.

2.2. Sample collection

In this study, a total of 150 measurements of water transparency were collected from Jezioro Kowalskie reservoir on 9 August 2018. Ninety measurements were taken in the main reservoir and 60 in the pre-reservoir (Fig. 1). Due to cloud cover in the part of the main reservoir, finally for analysis measuring points were selected from the pre-reservoir, characterized by higher variability of water transparency in comparison with the main part. To develop a quantitative relationship between field measurements and the Sentinel-2 sensor data, the field sampling day corresponded to the acquisition day of the satellite imagery. For the Secchi disk transparency (SDT) measurement, a standard black and white Secchi disk with a diameter of 0.2 m was used. The disk was lowered into the water and the depth when it was no longer visible was recorded. The water transparency was measured from a calibrated line. Data collection was carried out from 8:30 to 11.00 coordinated universal time (UTC), to obtain ground observation data during registration of the reservoir by the satellite, at the same time avoiding external factors such as wind and waves. Additionally, the measurements were always collected on the sun shaded side of the boat, simultaneously avoiding the boat and observer shadows on the water. The sampling site positions were determined with a global positioning system tracker (GPS GARMIN OREGON 300).

2.3. Satellite imagery

In order to fulfil the GMES mission requirements, ESA members decided to develop a complementary Sentinel satellite constellation for Earth observations. Sentinel-2 is a constellation of two satellites which are operating simultaneously, enabling effective and low-cost data collection. One of the basic objectives of the Sentinel-2 programme is to complement the SPOT (Satellite Pour l'Observation de la Terre) and Landsat missions in order to obtain a continuous, comparable data series. The orbit of Sentinel-2 is at 786 km altitude, and the satellites are phased at 180° to each other. The satellites Sentinel-2A and Sentinel-2B were launched on June 23, 2015 and on March 7, 2017 respectively. A sensing time of 10.30 a.m., as the most suitable for compromise between minimizing cloud cover and ensuring sun illumination (Drusch et al., 2012), was used. The main instrument of the satellite, Multi- Spectral Imager (MSI), is based on the pushbroom concept and provides imagery from 56°S (South America) to 83°N (Greenland) with a swath width of 290 km. The MSI sensor measures reflectance in 13 spectral bands from

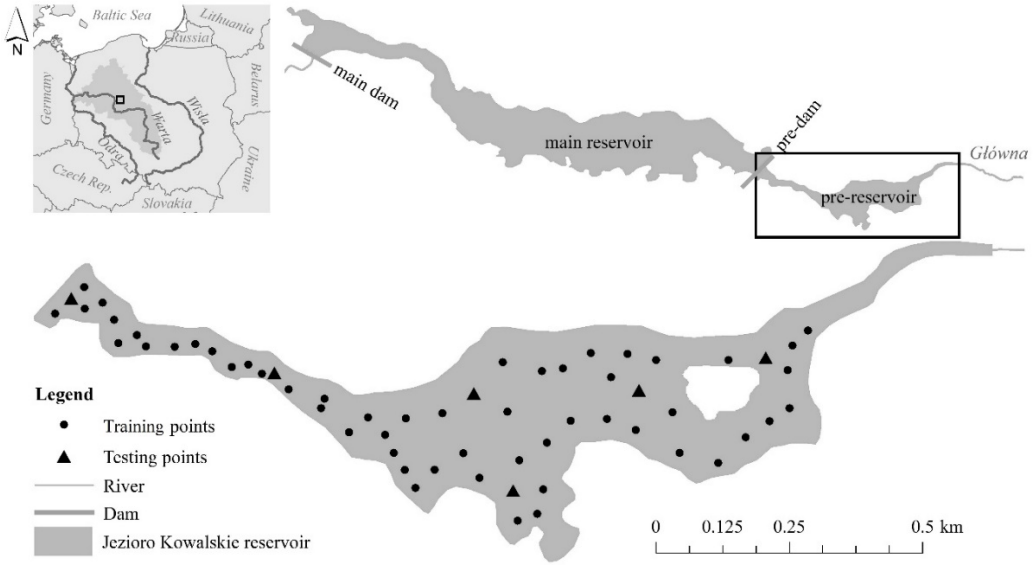

Figure 1. Sampling location in the Jezioro Kowalskie reservoir, Poland.

the visible (VIS) and near-infrared (NIR) to the short-wave infrared (SWIR) in resolution: 10 m (blue – B, green – G, red – R, near-infrared – NIR bands), 20 m (4 narrow bands for characterization of vegetation, 2 short wave infrared – SWIR bands) and 60 m (coastal aerosol, water vapour and cirrus detection bands). The revisit time of the Sentinel-2 constellation varies from 2-3 days (at mid latitudes) to 5 days (at the Equator).

Sentinel-2B, level 1C imagery (ID= L1C_T33UXU_A007441_20180809T100021) acquired on 9 August 2018 (10:00:21 UTC) was downloaded from the Sentinel Hub website (https://sentinel-hub.com/) in a tile of 100 km^2. Level 1C products are radiometrically and geometrically corrected (Top of Atmosphere – TOA), including orthorectification and spatial assignment to a global reference system (WGS84, EPSG:4326). In the first step, the Sentinel-2 satellite imagery composite was created. To scale the Sentinel-2 composite to surface reflectance, the Dark Object Subtraction (DOS) method was carried out (Chavez, 1988) in the Semi-Automatic Classification Plugin in QGIS software. The DOS is an atmospheric correction method, which is based on the assumption that some objects in the satellite imagery were under complete shadow during acquisition, their radiances are disturbed by atmospheric scattering and these pixels must have zero reflectance (Giardino et al., 2001; Chavez, 1996; Fernández-Manso et al., 2016). According to Lantzanakis et al., (2017), all analyzed correction methods (Second Simulation of Satellite Signal in the Solar Spectrum – 6S, Fast Line-of-sight Atmospheric Analysis of Hypercubes – FLAASH and DOS) perform results for water surfaces similarly. In the last processing step, the reflectance values of all bands were extracted from the Sentinel-2B composite.

2.4. Regression model development

In the first step, in-situ measurements were divided into two groups – training and test points. From 60 in-situ measurements in the pre-dam reservoir, 54 points were selected to build regression, while 6 points (10%) constituted a set of data for the test procedure. The training set of data contains 54 SDT measurements (2 pts/ha), where the distance between sample points varies from 19 to 113 m with the mean of 48 m. Mean Secchi disk transparency was 21 cm with the range of variation from 11 to 27 cm. The test set of data contains 6 SDT measurements (0.25 pts/ha), values of which were in the range of the training set. Additionally, test points were located in different parts of the reservoir, and the distance between sample points varies from 196 to 1665 m with a mean distance of 278 m. Mean Secchi disk transparency was 19 cm with the range of 14–23 cm. The mean distance between training and test points is 48 m, minimum 24 m and maximum 70 m.

In the second step, to build the regression model on the basis of Sentinel-2 imagery, all band reflectance values were extracted to the sampling points (Fig. 2). Paired reflectance values of satellite imagery and in-situ data were considered to develop the regression models for SDT estimation. For this purpose, a set of data containing 54 in-situ measurements and reflectance values of all Sentinel-2 bands was compiled. Then, several variables (Table 1) were used to determine the combination of satellite image bands characterized by the greatest significance with in-situ data based on the r^2 values. Finally, the model equation based on the blue and red band ratio (Blue/Red) represents the highest agreement in comparison with other variables and was used for SDT estimation. As a result, a total of 54 pairs of data (satellite and in-situ measurements) and 2717 reflectance values were used for development of the Secchi Disk Transparency image ($SDT_{Satellite}$). Mapping and SDT images were performed in ArcGIS 10.6.1. software

Table 1. Characteristics of Sentinel-2 products

Satellite	Bands used in final equations	References
Landsat 8	Green, Near Infrared	Al-Fahdawi et al., (2015)
Landsat 5, Landsat 7	Near Infrared	Bohn et al., (2018)
Landsat 5, Landsat 7	Blue, Near Infrared	Bonansea et al., (2015)
Landsat 4-5	Green, Red	Duan et al., (2009)
Landsat 5	Blue, Green	Giardino et al., (2001)
Landsat 5, Landsat 7	Blue, Red	McCullough et al., (2012)
Landsat 4, Landsat 5, Landsat 7	Blue, Red	Olmanson et al., (2014)
Landsat 5	Blue, Green	Rodríguez et al., (2014)
Landsat 8	Green, Red	Ren et al., (2018)
Landsat 5, Landsat 7	Blue, Green, Red	Sass et al., (2007)
MODIS, Landsat 5	Blue, Red	Wu et al., (2008)
Quickbird 2	Blue, Green, Red, Near Infrared	Yüzügüllü & Aksoy, (2011)

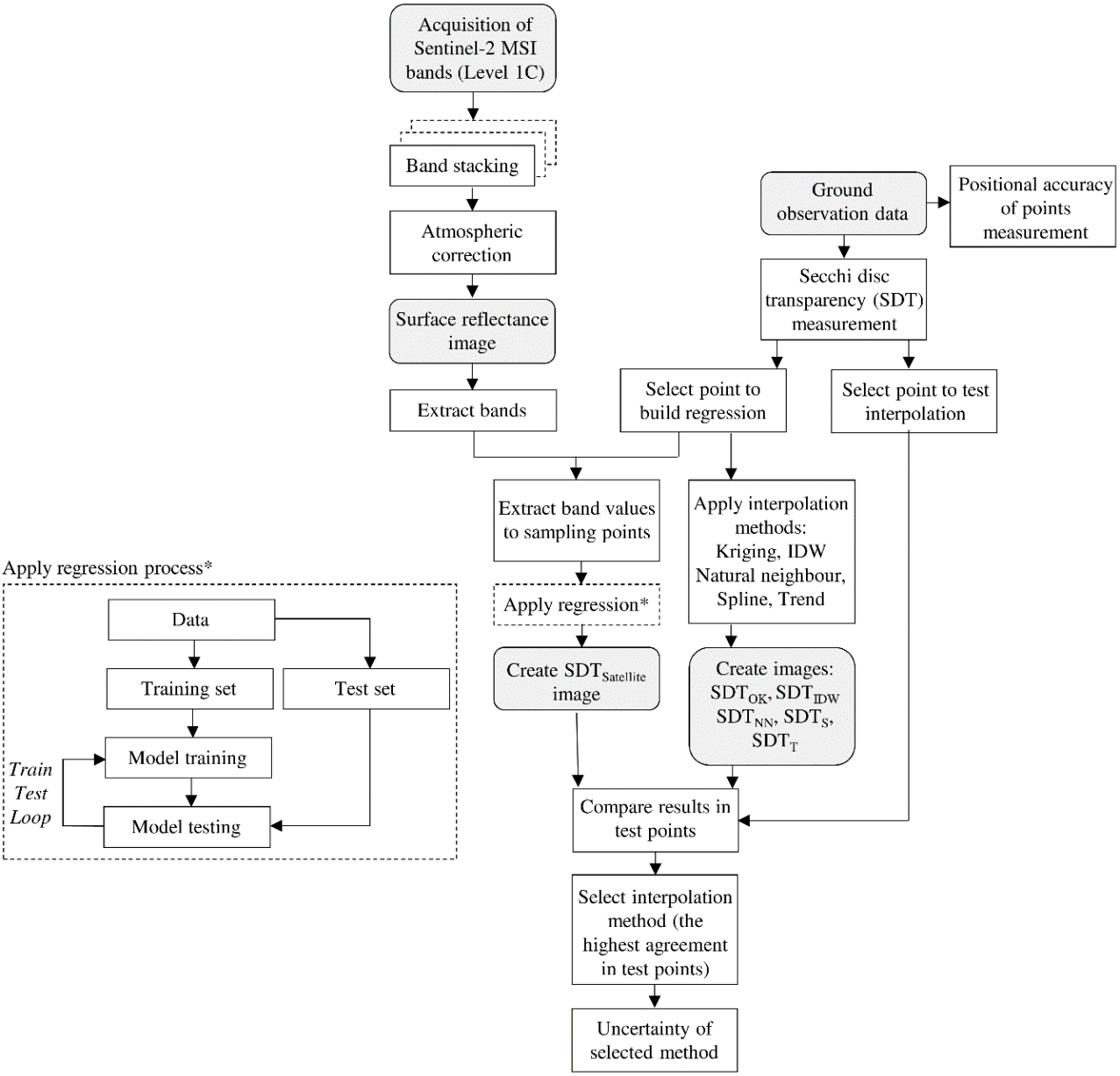

Figure 2. Methodology applied in this study.

2.5. Interpolation methods

In the third step to present the spatial variability of the water transparency in the pre-dam reservoir five worldwide interpolation methods implemented in ArcGIS 10.6.1 software were used. The Inverse Distance Weighting (IDW) interpolation is based on the assumption that the value at an unmeasured point Z_p can be approximated by a weighted average of observed values Z_i. The value Z_p at an unmeasured point is calculated in equation 1, where Z_i (i = 1,2,. . .,n) are the measured value at n points, and w_i are the weights given by:

$$Z_p = \sum_{i=1}^{n} w_i Z_i \quad (1)$$

$$w_i = \frac{d_i^{-p}}{\sum_{i=1}^{n} d_i^{-p}} \quad (2)$$

where d_i is the distance between the ith measured value Z_i and the unmeasured (predicted) point Z_p, and p is the power (exponent) variable. During the IDW interpolation, a power value of 2 and a search radius of 12 points were assumed.

The Natural Neighbour (NN) interpolation methods used the same formula as IDW. However, to select points for interpolation and compute the weights the Voronoi diagram is used. The weight *wi* of measured point *Zi* is expressed as:

$$w_i = \frac{S(r_i)}{\sum_{i=1}^{n} S(r_i)} \quad (3)$$

where $S(r_i)$ is the area of natural region *ri*; n is the

number of natural neighbours of unmeasured (interpolated) point Z_p.

The Spline (S) interpolation method estimates values at unmeasured points Z_p using a function that minimizes overall surface curvature, resulting in a smooth surface that passes exactly through the input points. The formula of SPLINE for surface interpolation is expressed as:

$$f(x,y)=T(x,y)+\sum_{i=1}^{n}\lambda_i R(d_i) \quad (4)$$

where n is the number of measured points; λ_i are coefficients calculated by the solution of a system of linear equations; di is the distance from the unmeasured point Z_p (x and y represented the location, i.e. the longitude and the latitude) to the ith measured point Z_i. To calculate $T(x,y)$ and $R(d_i)$ the Regularized option in ArcGIS was used. During the S interpolation, the weight value of 0.1 and 12 as the number of points were assumed.

The Trend (T) method is a statistical method using a global polynomial interpolation that enables one to find the surface that fits the measured points using least-squares regression fit. In this study to predict the value of unmeasured points the third-order interpolation is used as follows:

$$Z_p(x,y)= c_o+xc_1+yc_2+x^2c_3+xyc_4+y^2c_5+x^3c_6+x^2yc_7+xy^2c_8+y^3c_9 \quad (5)$$

where x and y represented the location (the longitude and the latitude) of the unmeasured points Zp and the c_n coefficient values are calculated using least-squares methods.

Kriging is an advanced interpolation procedure that uses the same general formula as IDW. However, the weights w_i are calculated by means of spatial autocorrelation analysis. This is done via a semivariogram, which represents the measured value spatial variation against the distance separating them. The values of the sample semivariogram are calculated from the equation:

$$\gamma(d)=\frac{1}{2m}\{Z(x_i)-Z(x_i+d)\}^2 \quad (6)$$

where m is the number of pairs of measured points separated by distance d, and $Z(x_i)$ and $Z(x_i + d)$ are the measured values at locations separated by distance d.

Finally the semivariogram was modelled by fitting a theoretical function to the sample semivariogram. In this study ordinary kriging (OK) using spherical model with search radius settings being 12 as the number of points and maximum distance of 1000 m.

To estimate spatial variation of Secchi disk transparency (SDT), the interpolation methods were applied: Ordinary Kriging (OK), Inverse Distance Weighted (IDW), Natural neighbour (NN), Spline (S) and Trend (T). On the basis of the selected interpolation method, five SDT images were created (SDT_{OK}, SDT_{IDW}, SDT_{NN}, SDT_S, SDT_T).

2.6. Assessment of interpolation methods

To select the interpolation method characterized by the highest agreement with in-situ measurements, obtained results were compared with transparency in test points. Statistical analyses based on linear and non-linear regressions were calculated using Statistica 13 software. To investigate the strength of the relationship between measured and predicted SDT values, the coefficient of determination (r^2) was used. The statistical hypothesis test was conducted at the significance level of 0.05. For the accuracy analysis of the spatial extrapolation methods, the mean absolute error (MAE), mean square error (MSE), and root-mean-square error (RMSE) were calculated as:

$$MAE= \frac{1}{N}\sum_{i=1}^{N}\left|\frac{Z_{SD\ measured,\ i}- Z_{SD\ derived,\ i}}{Z_{SD\ measured,\ i}}\right| \quad (7)$$

$$MSE= \frac{1}{N}\sum_{i=1}^{N}\left(Z_{SD\ measured,\ i}- Z_{SD\ derived,\ i}\right)^2 \quad (8)$$

$$RMSE= \sqrt{\frac{1}{N}\sum_{i=1}^{N}\left(Z_{SD\ measured,\ i}- Z_{SD\ derived,\ i}\right)^2} \quad (9)$$

where N is the number of in-situ measurements, and $Z_{SD\ measured}$ and $Z_{SD\ derived}$ are Secchi disk depths from in-situ measurement and calculated on the basis of the interpolation method.

Table 2. Characteristic values of Sentinel-2 bands used in this study.

Sentinel-2 bands	Training set (N= 54)	Test set (N= 6)	Pre-reservoir area
B2 (Blue)	0.022 – 0.029 0.025 – 0.001	0.023 – 0.027 0.025 – 0.001	0.016 – 0.051 0.025 – 0.002
B3 (Green)	0.033 – 0.041 0.037 – 0.002	0.038 – 0.039 0.038 – 0.001	0.019 – 0.065 0.037 – 0.004
B4 (Red)	0.032 – 0.036 0.034 – 0.001	0.033 – 0.035 0.034 – 0.001	0.021 – 0.090 0.035 – 0.003
B8 (Near Infrared)	0.024 – 0.041 0.033 – 0.004	0.026 – 0.044 0.034 – 0.006	0.024 – 0.418 0.080 – 0.091
B2/B4	0.654 – 0.817 0.732 – 0.036	0.660 – 0.779 0.737 – 0.045	0.500 – 0.917 0.717 – 0.044

(minimum-maximum, mean-standard deviation)

Finally, in order to determine the uncertainty of the selected interpolation method in different parts of the reservoir, 50 different combinations of data sets (training and test) were selected. On the basis of spatial differences between data sets, the basic statistics were calculated in each of 2717 pixel central points (minimum, maximum, mean, standard deviation, range). Spatial distribution of statistical characteristics allows one to indicate parts of the reservoir characterized by the highest uncertainty of interpolation method supported by the satellite imagery.

3. RESULTS

Characteristic values of Sentinel-2 single bands and combination of blue and red bands are presented in Table 2. The minimum value of the B2/B4combination in the training set of data was 0.654, while the maximum was 0.817. The mean value (±standard deviation) was 0.732 ± 0.036. Characteristic values of combination Sentinel-2 bands in the test set are in the range of the training set. SDT values ranged from 0.660 to 0.779, with a mean value (±standard deviation) of 0.737 ± 0.045 in the test dataset. Values of applied regression for the whole pre-dam reservoir area varies from 0.500 to 0.917, with the mean value (±standard deviation) of 0.717 ± 0.044.

The scatterplot (Fig. 3a) shows the relation between measured SDT and the variable based on the blue and red satellite band (B2/B4). The regression relationship of the function between the paired band-ratio equation and measured SDT for the training dataset is characterized by the coefficient of determination equal to 0.830 ($p<0.001$). The applied model performed well in the test dataset (Fig. 3b). Measured and derived SDT values were disturbed along the 1:1 line, which indicates that the adopted algorithm could be successfully used to estimate Secchi disk transparency in Jezioro Kowalskie reservoir. The coefficient of determination for delivered and in-situ measured SDT is 0.844 ($p<0.05$).

Spatial changes of water transparency estimated by applied interpolation methods are presented in Figure 4. The largest differences between interpolation methods in the test dataset occur at points no. 5 and 6, which is equals to 11 and 12 cm, respectively. The points are located near the small island in the eastern part of the pre-dam reservoir. The minimum values at point no. 5 are characterized by the interpolation method based on satellite imagery (12 cm), while the highest is estimated by the Natural Neighbour method (23 cm). SDT values measured in this location during in-situ collection of data are equal to 14 cm. The minimum SDT values at point no. 6 are characterized by the Ordinary Kriging and Trend methods (20 cm), while the highest is estimated by the Spline method (31 cm). SDT measured in this location during in-situ collection of data is 23 cm; the same SDT value was obtained on the basis of the interpolation method based on satellite imagery. The smallest differences between interpolation methods occur at points no. 1 and 2, equalling 4 and 6 cm, respectively. SDT values measured in these locations are 22 and 21 cm. The highest agreement with in-situ measurement is characterized by the method based on satellite imagery, the derived SDT values equalling 22 and 21 cm also (Fig. 4).

Figure 5 summarizes the variations of Secchi disk transparency based on in-situ measurements and interpolation methods. The model applied on the basis of the Sentinel-2 band-ratio equation shows a median SDT value of 20 cm with the range of variation 12-23 cm. SDT derived from Ordinary Kriging method varies from 19 to 22 cm with a median value of 20 cm.

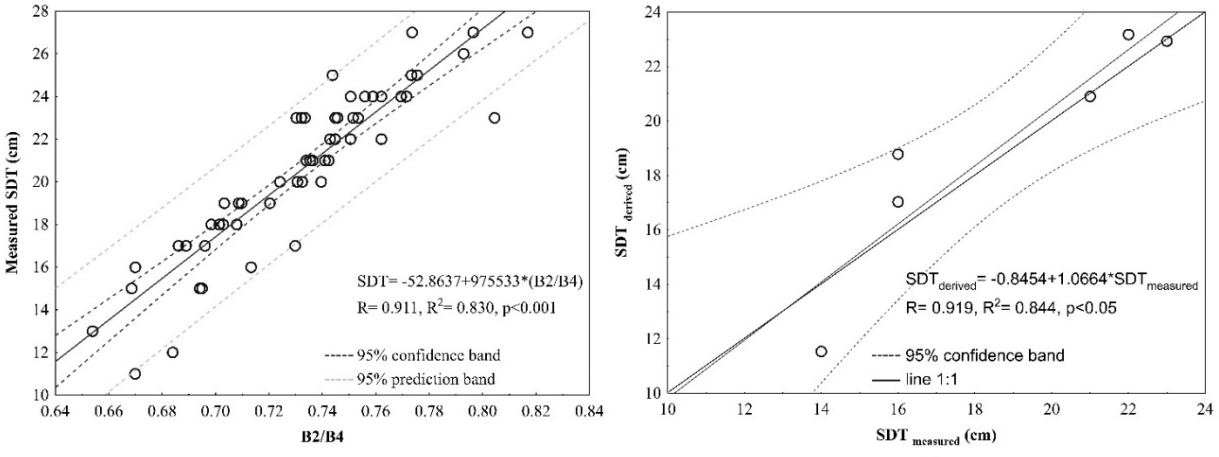

a b

Figure 3. Relationship between measured Secchi Disk Transparency (SDT) and (a) blue/red band reflectance of Sentinel-2 data and (b) derived SDT in the Jezioro Kowalskie reservoir, Poland.

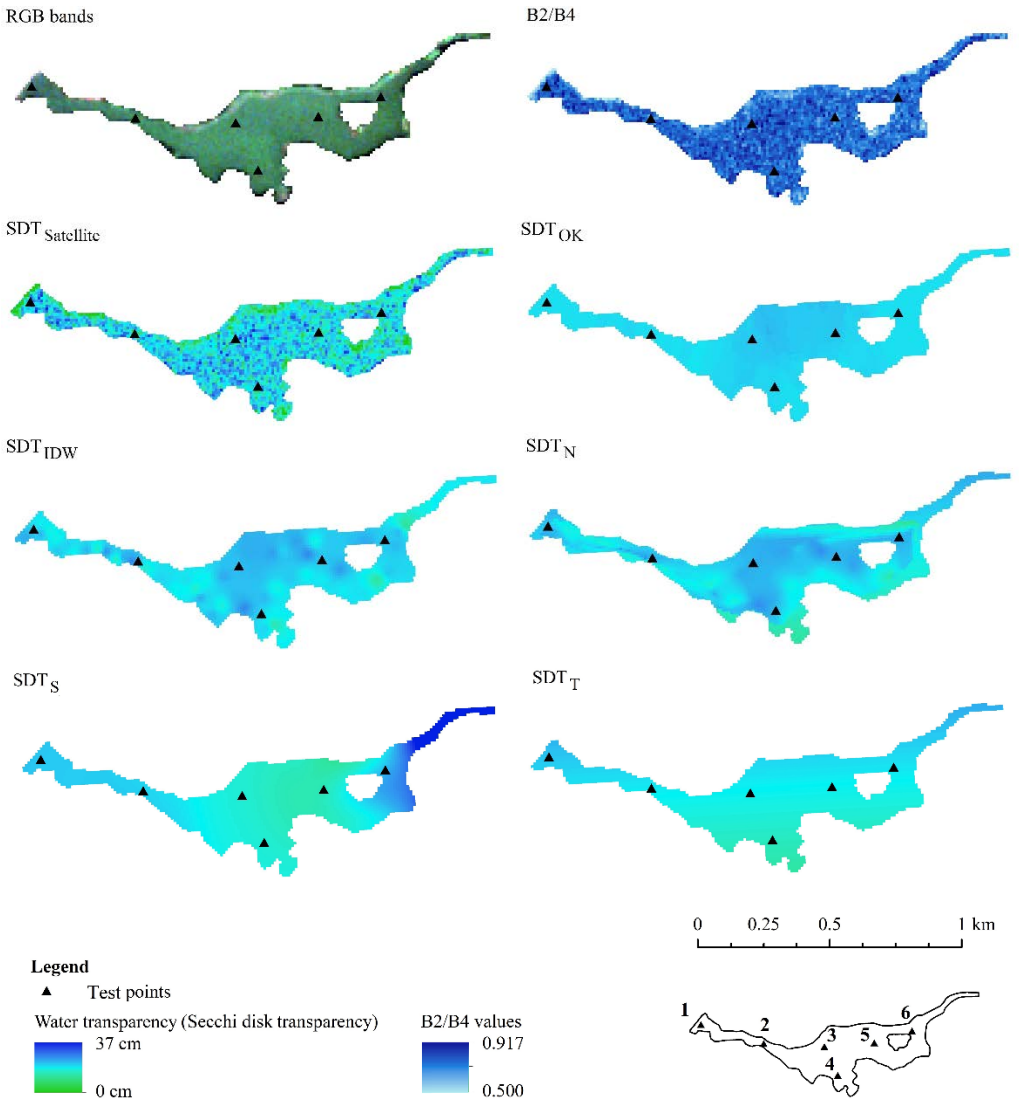

Figure 4. Spatial changes of water transparency estimated by applied interpolation methods in the Jezioro Kowalskie reservoir, Poland.

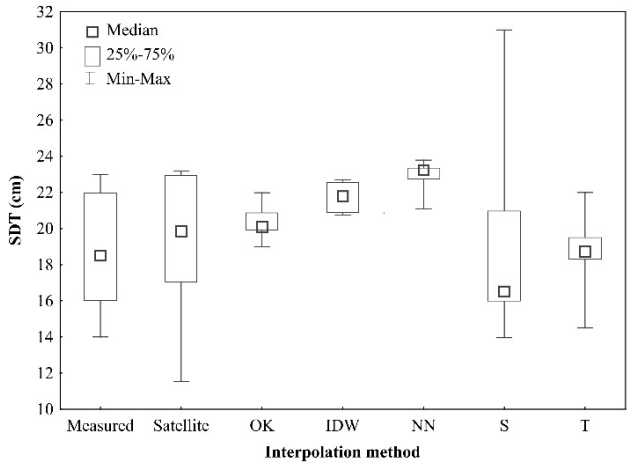

Figure 5. Secchi disk transparency (SDT) estimated on the basis of applied interpolation methods.

Estimation of SDT based on the Inverse Distance Weighted method allows one to predict an SDT value from 21 to 23 cm, while the median value is 22. The highest median value was obtained on the basis of Natural Neighbour and was 23 cm with the range of variation 21-24 cm. SDT derived from the Spline method varies from 14 to 31 cm with a median value of 17 cm. The model applied on the basis of the Trend method shows a median SDT value of 19 cm with the range of variation 14-22 cm (Fig. 5).

The highest coefficient of determination in the test dataset was obtained for the interpolation method based on satellite imagery and was 0.844 ($p<0.05$), while the lowest was 0.030 for the IDW method (Table 2). According to Rufo et al., (2018), the mean absolute error (MAE) is used to detect bias; it should be 0 when estimated values are equal to those measured. In this study, the MAE values are similar and equal to 17 and 18, regardless of the adopted interpolation method. The lowest mean square error (MSE) was obtained for interpolation method based on satellite imagery and was 3, while the highest was 33 for the Natural Neighbour method. The root-mean-square error (RMSE) is used to

compare predicted values based on different interpolation methods with the measured values; if RMSE equals 0 it means that the predicted values are the same as the measured ones (Rufo et al. 2018). In this study, the lowest RMSE value was obtained for the model applied on the basis of the Sentinel-2 band-ratio equation and was 1.65. The highest RMSE value was 5.77 and was obtained for the Natural Neighbour method (Table 3).

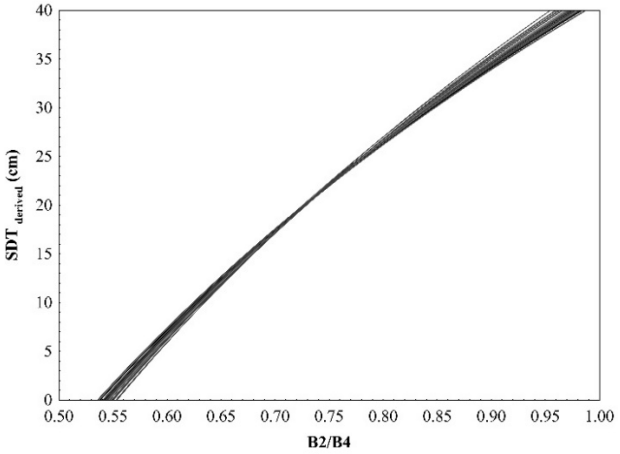

Figure 6. Relationship between 50 variants of derived Secchi Disk Transparency (SDT) and blue/red band reflectance of Sentinel-2 data in the Jezioro Kowalskie reservoir, Poland.

In order to determine the uncertainty of the model applied on the basis of the Sentinel-2 band-ratio equation, 50 different combinations of datasets (training and test) were selected. The coefficient of determination varies from 0.763 to 0.935 with the mean value of 0.835. Training datasets are compiled in Figure 6. In this study, the quotient of blue and red band varies from 0.654 to 0.817 (Table 2). Model prediction in this range is characterized by the highest stability; the maximum difference between training datasets occurs in the boundary of the dataset and is less than 2 cm. The uncertainty of the derived SDT values is higher beyond the boundaries of the developed model.

In order to indicate parts of the reservoir characterized by the highest uncertainty of predicted SDT values, the spatial distribution of differences between 50 combinations of datasets were calculated (Fig. 7). The analysis was carried out for each of 2717 pixel central points from the Sentinel-2 satellite. Standard deviations vary from 0.0 to 0.7. The results show that more than 91% of the reservoir is characterized by a standard deviation less than 0.2, while only 0.25% shows values higher than 0.5. The highest standard deviations occur near the shoreline of the reservoir and the dam. It might be related to the small depth of water and the possibility of spectral reflection from the bottom of the reservoir. Additionally, there are wooded areas next to the reservoir shoreline which may have an influence on the reflectance signal from the satellite sensor. The difference between minimum and maximum values (range) in most of the reservoir (98%) is less than 1 cm.

Table 3. Characteristic values of Sentinel-2 bands used in this study.

Interpolation method	R	R^2	p	MAE	MSE	RMSE
Satellite	0.919	0.844	0.009	18	3	1.65
Kriging	-0.764	0.584	0.077	18	20	4.51
IDW	-0.173	0.030	0.743	17	23	4.78
Natural Neighbour	-0.434	0.189	0.389	17	33	5.77
Spline	0.757	0.574	0.081	18	15	3.85
Trend	0.635	0.403	0.176	18	7	2.67

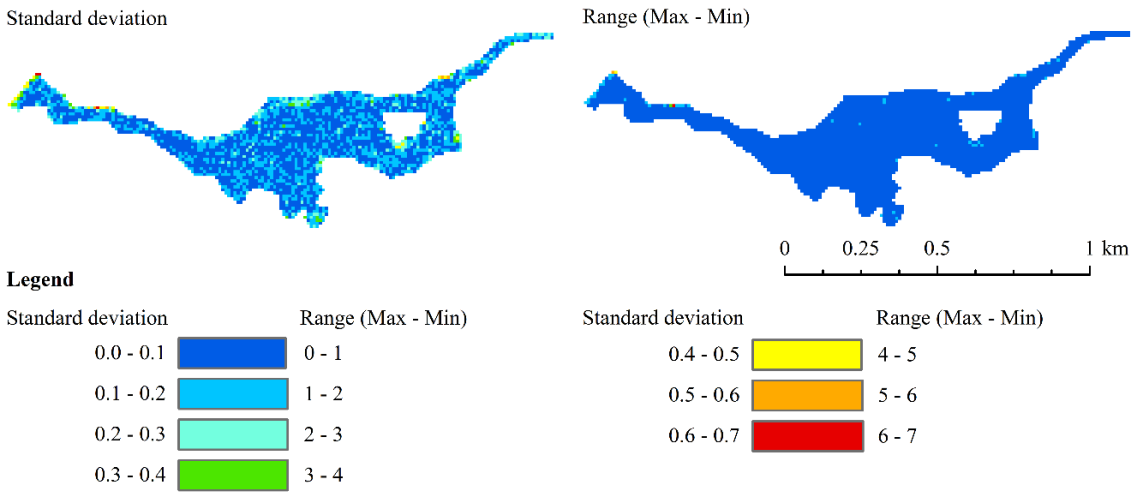

Figure 7. Spatial characteristics of standard deviation and range on the basis of 50 variants of derived Secchi Disk Transparency (SDT).

4. DISCUSSION

The main objective of this study was to apply the satellite imagery for estimating water transparency. Additionally, various interpolation methods were used to deliver Secchi disk transparency (SDT). The methods were tested against in-situ measurements conducted in the Jezioro Kowalskie reservoir. In this study, the most common interpolation techniques were used: Kriging, IDW, Natural Neighbour, Spline and Trend methods. Shen et al., (2019) stated that Ordinary Kriging is an interpolation method with moderately acceptable accuracy, while IDW decreased the accuracy for environmental analyses. In turn, Gong et al., (2014) reported that accuracy between measured and estimated values was higher with the IDW method than Kriging. Some of the interpolation methods are still not well recognized for environmental analysis applications such as the Spline or Trend method. The results in this study confirm the conclusion of Shen et al., (2019) and Bhunia et al., (2016) that Kriging is superior to the IDW interpolation method, which has the worst accuracy. However, due to the differences of accuracy depending on interpolation methods in previous studies, it is still inconsistent which interpolation method is more accurate than another. The results show that the method based on satellite imagery is characterized by the highest accuracy and can be retrieved to assess water transparency in reservoirs. The high correlation between in-situ measurements and remote sensing data has been confirmed in many studies (Dörnhöfer et al., 2018a, Cannizzaro et al., 2008, Yadav et al., 2017). In comparison with other satellites (Al-Fahdawi et al., 2015, Bohn et al., 2018, Wu et al., 2008), the Sentinel-2 provides non-cost products with unprecedented spatial and temporal resolution. It makes it possible to estimate Secchi disk transparency as data with a spatial resolution equal to 10 m. The paper concludes that applying the interpolation method based on satellite imagery could be an economical and feasible solution for mapping Secchi disk depth in inland waters. Ren et al., (2018) and Wu et al., (2008) developed a reliable standard equation to predict water transparency in lakes based on satellite data only. However, comparing the RMSE and MEA values for the same equation calculated in several studies shows large differences. It confirms that developing a single equation for remotely sensed water clarity is still uncertain, but at the same time its usefulness for monitoring of aquatic environments is undeniable (Alikas & Kratzer, 2017). According to Butt & Nazeer (2015), improved techniques of atmospheric correction could have an increasing impact on developing a reliable standard equation. For example, Kratzer & Vinterhav (2010) show that MEGS atmospheric correction was characterized as a more accurate technique than FUB and C2R. In this study, the DOS method was selected, which could have an impact on disturbance of results on the basis of standard algorithms. However, Lantzanakis et al., (2017) showed that several correction methods (6S, FLAASH and DOS) achieve similar results for water surfaces. Higher errors of the standard equations could be caused by rare specific phenomena also, for example an exceptional bloom of *Chrysochromulina* spp. in the whole Baltic Sea (Kratzer & Vinterhav 2010) or in Himmerfjärden bay (Kratzer et al., 2008). Previous studies (Sojka et al., 2016, Sojka et al., 2017) confirm that Jezioro Kowalskie is exposed to algal bloom phenomena and eutrophication, especially in the pre-dam zone. During in-situ measurements for this study, this part of the reservoir was characterized by lower water transparency in comparison with the main part due to the high concentration of phytoplankton. Various factors (defined above) which have an impact on the accuracy of standard equations makes it necessary to search for a methodology adapted to a particular analysis. One of the most promising solutions seems to be building regression models between variables of satellite imagery band values and in-situ measurements, separately for each analysis. This study shows that the most accurate variable seems to be the blue and red band quotient (Blue/Red), which was also noted in previous studies (Kloiber et al., 2002, Urbański et al., 2016). Building of independent equations based on satellite imagery is characterized by higher accuracy than standard equations. Obtained results show that the highest values occur near the shoreline of the reservoir, which can be related to overgrowth areas or small depth water. In these places the spectral reflectance value may be disrupted by plants and the bottom of the reservoir. The methodology was applied for the reservoir characterized by high concentration of algae blooms, which is one of the biggest problems for lowland reservoirs. Despite small depth in pre-reservoir, during in-situ measurements the bottom was invisible due to low water transparency. In authors opinion, methodology for reservoirs with disrupted reflectance data by bottom should be further developed. In this case, in-situ data should be collected in clear reservoirs characterized by high water transparency in months where vegetation process has already started. It will provide information about possibility using semi-automatic equations in water bodies with diverse water transparency.

According to the authors, the main disadvantage of the applied methodology to estimate Secchi disk transparency is the fact that each analysis

requires its own equation. Additionally, this semi-automatic methodology requires in-situ measurements which will be representative for the whole range of water transparency. The determination of in-situ measurement locations is crucial for a comprehensive overview of the Secchi disk transparency.

5. CONCLUSION

The conducted research allowed the following specific conclusions to be formulated:

- individual regression models created on the basis of satellite imagery allow higher accuracy of assessment of the water transparency in reservoirs compared to commonly used interpolation methods based on GIS (Kriging, IDW, Natural Neighbour, Spline, Trend).
- The highest accuracy variable to estimate Secchi disk transparency on the basis of satellite data is the blue and red band ratio (Blue/Red).
- The highest uncertainty of the obtained results occurs near the shoreline of the reservoir and near the dam. It might be related to overgrowth areas or small depth water and the possibility of spectral reflection from plants and the bottom of the reservoir. Additionally, it might be related to wooded areas near the reservoir shoreline which can have an influence on the reflectance signal from the satellite sensor.
- The highest uncertainty associated with the applied individual regression occurs in the case of limit values of the B2/B4 ratio, which were not used during regression model development.
- The major limitation of using Sentinel-2 data is cloud coverage, which significantly reduces the number of observations and accuracy of the developed model.
- Future studies should be carried out to determine how big the set of in-situ measurements should be to obtain highly accurate interpolation.

REFERENCES

Agutu, N.O., Awange, J.L., Zerihun, A., Ndehedehe C.E., Kuhn M. & Fukuda Y., 2017. *Assessing multi-satellite remote sensing, reanalysis, and land surface models' products in characterizing agricultural drought in East Africa.* Remote Sensing of Environment, 194, 287-302.

Al-Fahdawi, A.A., Rabee, A.M. & Al-Hirmizy, S.M., 2015. *Water quality monitoring of Al-Habbaniyah Lake using remote sensing and in situ measurements.* Environmental Monitoring and Assessment, 187, 6, 367.

Alikas, K. & Kratzer, S., 2017. *Improved retrieval of Secchi depth for optically-complex waters using remote sensing data.* Ecological Indicators, 77, 218-227.

Aschbacher, J. & Milagro-Pérez, M.P., 2012. *The European Earth monitoring (GMES) programme: Status and perspectives.* Remote Sensing of Environment, 120, 3-8.

Bhunia, G.S., Shit, P.K. & Maiti, R., 2016. *Comparison of GIS-based interpolation methods for spatial distribution of soil organic carbon (SOC).* Journal of the Saudi Society of Agricultural Sciences, 17, 2, 114-126.

Bogdał, A., Policht-Latawiec, A. & Kołdras, S., 2015. *Changes of water quality indices with depth at drinking water intake from Dobczyce Reservoir.* Annual Set the Environment Protection, 17, 2, 1239-1258.

Bohn, V.Y., Carmona, F., Rivas, R., Lagomarsino, L., Diovisalvi, N. & Zagarese, H.E., 2018. *Development of an empirical model for chlorophyll-a and Secchi Disk Depth estimation for a Pampean shallow lake (Argentina).* The Egyptian Journal of Remote Sensing and Space Science, 21, 2, 183-191.

Bonansea, M., Rodriguez, M. C., Pinotti, L. & Ferrero, S., 2015. *Using multi-temporal Landsat imagery and linear mixed models for assessing water quality parameters in Río Tercero reservoir (Argentina).* Remote Sensing of Environment, 158, 28-41.

Borek, Ł., 2018. *Eutrophication risk of water in the manor-park channels: different ways of evaluation.* Carpathian Journal of Earth and Environmental Sciences, 13, 2, 409-421.

Bus, A., & Mosiej, J., 2018. *Water quality changes of inflowing and outlawing water from complex of Niewiadoma Reservoirs located at Cetynia River.* Annual Set the Environment Protection, 20, 1793-1810.

Butt, M.J. & Nazeer, M., 2015. *Landsat ETM+ Secchi Disc Transparency (SDT) retrievals for Rawal Lake, Pakistan.* Advances in Space Research, 56, 7, 1428-1440.

Cannizzaro, J.P., Carder, K.L., Chen, F.R., Heil, C.A. & Vargo, G.A., 2008. *A novel technique for detection of the toxic dinoflagellate, Karenia brevis, in the Gulf of Mexico from remotely sensed ocean color data.* Continental Shelf Research, 28, 1, 137-158.

Cavalli, R.M., Laneve, G., Fusilli, L., Pignatti, S. & Santini F., 2009. *Remote sensing water observation for supporting Lake Victoria weed management.* Journal of Environmental Management, 90, 7, 2199-2211.

Chavez, P.S., 1988. *An improved dark-object subtraction technique for atmospheric scattering correction of multispectral data.* Remote Sensing of Environment, 24, 3, 459-479.

Chavez, P.S., 1996. *Image-based atmospheric corrections-revisited and improved.* Photogrammetric Engineering and Remote

Sensing, 62, 9, 1025-1035.

Chawira, M., Dube, T. & Gumindoga, W., 2013. *Remote sensing based water quality monitoring in Chivero and Manyame lakes of Zimbabwe.* Physics and Chemistry of the Earth, 66, 38-44.

Dąbrowska, J., Dąbek, P.B. & Lejcuś, I., 2018. *A GIS based approach for the mitigation of surface runoff to a shallow lowland reservoir.* Ecohydrology & Hydrobiology, In Press.

Dąbrowska, J., Lejcuś, K., Kuśnierz, M., Czamara, A., Kamińska, J. & Lejcuś, I., 2016. *Phosphate dynamics in the drinking water catchment area of the Dobromierz Reservoir.* Desalination and Water Treatment, 57, 53, 25600-25609.

Dlamini, S., Nhapi, I., Gumindoga, W., Nhiwatiwa, T. & Dube T., 2016. *Assessing the feasibility of integrating remote sensing and in-situ measurements in monitoring water quality status of Lake Chivero, Zimbabwe.* Physics and Chemistry of the Earth, Parts A/B/C, 93, 2-11.

Donlon, C., Berruti, B., Buongiorno, A., Ferreira, M.H., Féménias, P., Frerick, J., Goryl, P., Klein, U., Laur, H., Mavrocordatos., C., Nieke, J., Rebhan, H., Seitz, B., Stroede, J. & Sciarra, R., 2012. *The Global Monitoring for Environment and Security (GMES) Sentinel-3 mission.* Remote Sensing of Environment, 120, 37-57.

Dörnhöfer, K., Klinger, P., Heege, T. & Oppelt, N., 2018a. Multi-sensor satellite and in situ monitoring of phytoplankton development in a eutrophic-mesotrophic lake. *Science of The Total Environment*, 612, 1200-1214.

Dörnhöfer, K., Scholze, J., Stelzer, K. & Oppelt, N., 2018b. *Water colour analysis of Lake Kummerow using time series of remote sensing and in situ data.* PFG–Journal of Photogrammetry, Remote Sensing and Geoinformation Science, 86, 2, 103-120.

Drusch, M., Del Bello, U., Carlier, S., Colin, O., Fernandez, V., Gascon, F., Hoersh, B., Isola, C., Laberinti, P., Martimort, P., Meygret, A., Spoto, F., Sy, O., Marchese, F. & Bargellini, P., 2012. *Sentinel-2: ESA's optical high-resolution mission for GMES operational services.* Remote Sensing of Environment, 120, 25-36.

Duan, H., Ma, R., Zhang, Y. & Zhang, B., 2009. *Remote-sensing assessment of regional inland lake water clarity in northeast China.* Limnology, 10, 135–141.

ESRI, 2012. *An Overview of the Interpolation Toolset.* (online: http://help.arcgis.com/en/arcgisdesktop/10.0/help/index.html#/An_overview_of_the_Interpolation_tools/009z00000069000000/, access on: 17.11.2018).

Fernández-Manso, A., Fernández-Manso, O. & Quintano, C., 2016. *Sentinel-2A red-edge spectral indices suitability for discriminating burn severity.* International Journal of Applied Earth Observation and Geoinformation, *50*, 170-175.

Fleming-Lehtinen, V. & Laamanen, M., 2012. *Long-term changes in Secchi depth and the role of phytoplankton in explaining light attenuation in the Baltic Sea.* Estuarine, Coastal and Shelf Science, 102, 1-10.

Giardino, C., Pepe, M., Brivio, P.A., Ghezzi, P. & Zilioli, E., 2001. *Detecting chlorophyll, Secchi disk depth and surface temperature in a sub-alpine lake using Landsat imagery.* Science of the Total Environment, 268, 1-3, 19-29.

Gong, G., Mattevada, S. & O'bryant, S.E., 2014. *Comparison of the accuracy of kriging and IDW interpolations in estimating groundwater arsenic concentrations in Texas.* Environmental Research, 130, 59-69.

Hestir, E.L., Brando, V.E., Bresciani, M., Giardino, C., Matta, E., Villa, P. & Dekker A.G., 2015. *Measuring freshwater aquatic ecosystems: The need for a hyperspectral global mapping satellite mission.* Remote Sensing of Environment, 167, 181-195.

Hicks, B.J., Stichbury, G.A., Brabyn, L.K., Allan, M.G. & Ashraf, S., 2013. *Hindcasting water clarity from Landsat satellite images of unmonitored shallow lakes in the Waikato region, New Zealand.* Environmental Monitoring and Assessment, 185, 9, 7245–7726.

Hydroprojekt, 2004. *The Jezioro Kowalskie reservoir in the Główna river: Water management rules – update*. Poznań.

Jaskuła, J., Sojka, M. & Wicher-Dysarz, J., 2018. *Analysis of the vegetation process in a two-stage reservoir on the basis of satellite imagery – a case study: Radzyny Reservoir on the Sama River.* Annual Set The Environment Protection, 20, 203-220.

Kim, D., Eum, H.I., Kaluarachchi, J.J. & Chun, J.A., 2019. *A sensitivity-based analysis for managing storage capacity of a small agricultural reservoir under drying climate.* Agricultural Water Management, 213, 410-418.

Kloiber, S.M., Brezonik, P.L. & Bauer, M.E., 2002. *A procedure for regional lake water clarity assessment using Landsat multispectral data.* Remote Sensing of Environment, 82, 1, 38-47.

Kratzer, S. & Vinterhav, C., *2010. Improvement of MERIS level 2 products in Baltic Sea coastal areas by applying the Improved Contrast between Ocean and Land processor (ICOL)-data analysis and validation.* Oceanologia, 52, 2, 211-236.

Kratzer, S., Brockmann, C. & Moore, G., 2008. *Using MERIS full resolution data to monitor coastal waters—A case study from Himmerfjärden, a fjord-like bay in the northwestern Baltic Sea.* Remote Sensing of Environment, 112, 5, 2284-2300.

Lantzanakis, G., Mitraka, Z. & Chrysoulakis, N., 2017. *Comparison of physically and image based atmospheric correction methods for Sentinel-2 satellite imagery.* In Perspectives on Atmospheric Sciences, Springer, Cham, 255-261.

Laurent, V.C., Schaepman, M.E., Verhoef, W., Weyermann, J. & Chávez, R.O., 2014. *Bayesian*

object-based estimation of LAI and chlorophyll from a simulated Sentinel-2 top-of-atmosphere radiance image. Remote Sensing of Environment, 140, 318-329.

Lee, Z., Shang, S., Hu, C., Du, K., Weidemann, A., Hou, W., Lin, J. & Lin, G., 2015. *Secchi disk depth: A new theory and mechanistic model for underwater visibility*. Remote Sensing of Environment, 169, 139-149.

Li, Y., Zhang, Y., Shi, K., Zhu, G., Zhou, Y., Zhang, Y. & Guo, Y., 2017. *Monitoring spatiotemporal variations in nutrients in a large drinking water reservoir and their relationships with hydrological and meteorological conditions based on Landsat 8 imagery.* Science of the Total Environment, 599, 1705-1717.

Liang, C.P., Chen, J.S., Chien, Y.C. & Chen, C.F., 2018. *Spatial analysis of the risk to human health from exposure to arsenic contaminated groundwater: A Kriging approach.* Science of The Total Environment, 627, 1048-1057.

Majozi, N.P., Salama, M.S., Bernard, S., Harper, D.M. & Habte M.G., 2014. *Remote sensing of euphotic depth in shallow tropical inland waters of Lake Naivasha using MERIS data*. Remote Sensing of Environment, 148, 178-189.

Martins, V.S., Kaleita, A., Barbosa, C.C., Fassoni-Andrade, A.C., de Lucia Lobo, F. & Novo, E.M., 2018. *Remote sensing of large reservoir in the drought years: Implications on surface water change and turbidity variability of Sobradinho reservoir (Northeast Brazil).* Remote Sensing Applications: Society and Environment, 13, 275-288.

McCullough, I.M., Loftin, C.S. & Sader, S.A., 2012. *Combining lake and watershed characteristics with Landsat TM data for remote estimation of regional lake clarity*. Remote Sensing of Environment, 123, 109-115.

Nishijima, W., Umehara, A., Sekito, S., Okuda, T. & Nakai, S., 2016. *Spatial and temporal distributions of Secchi depths and chlorophyll a concentrations in the Suo Nada of the Seto Inland Sea, Japan, exposed to anthropogenic nutrient loading*. Science of The Total Environment, 571, 543-550.

Odermatt, D., Pomati, F., Pitarch, J., Carpenter, J., Kawka, M., Schaepman, M. & Wüest A., 2012. *MERIS observations of phytoplankton blooms in a stratified eutrophic lake.* Remote Sensing of Environment, 126, 232-239.

Olmanson, L.G., Brezonik, P.L. & Bauer, M.E., 2014. *Geospatial and temporal analysis of a 20-year record of Landsat-based water clarity in Minnesota's 10,000 lakes.* Journal of the American Water Resources Association 50, 3, 748–761.

Pekel, J.F., Cottam, A., Gorelick, N. & Belward, A.S., 2016. *High-resolution mapping of global surface water and its long-term changes.* Nature, 540, 418-422.

Philippart, C.J., Salama, M.S., Kromkamp, J.C., van der Woerd, H.J., Zuur, A.F. & Cadée, G.C., 2013. *Four decades of variability in turbidity in the western Wadden Sea as derived from corrected Secchi disk readings.* Journal of Sea Research, 82, 67-79.

Policht-Latawiec, A., Bogdał, A., Kanownik, W., Kowalik, T., Ostrowski, K. & Gryboś, P., 2014. *Quality and usable values of small flysch river water.* Annual Set the Environment Protection, 16, 1, 546-561.

Regional Inspectorate of Environmental Protection, 2016. *Classification of rivers water quality parameters in the Wielkopolskie voivodship in the year 2015 – Główna – Borowo Młyn* (online: http://poznan.wios.gov.pl/wios/ocena2016/rzeki/Glowna-Borowo_Mlyn.pdf, access on: 09.11.2018).

Ren, J., Zheng, Z., Li, Y., Lv, G., Wang, Q., Lyu, H., Huang, C., Liu, G., Du, C., Mu, M., Lei, S. & Bi, S., 2018. *Remote observation of water clarity patterns in Three Gorges Reservoir and Dongting Lake of China and their probable linkage to the Three Gorges Dam based on Landsat 8 imagery.* Science of the Total Environment, 625, 1554-1566.

Rodríguez, Y.C., El Anjoumi, A., Gómez, J.D., Pérez, D.R. & Rico, E., 2014. *Using Landsat image time series to study a small water body in Northern Spain*. Environmental Monitoring and Assessment, 186, 6, 3511-3522.

Rufo, M., Antolín, A., Paniagua, J. M. & Jiménez, A., 2018. *Optimization and comparison of three spatial interpolation methods for electromagnetic levels in the AM band within an urban area*. Environmental Research, 162, 219-225.

Sass, G.Z., Creed, I.F., Bayley, S.E. & Devito, K.J., 2007. *Understanding variation in trophic status of lakes on the Boreal Plain: a 20 year retrospective using Landsat TM imagery*. Remote Sensing of Environment, 109, 2, 127-141.

Sender, J., Garbowski, M., Urban, D. & Demetraki-Paleolog, A., 2018. *Preliminary study for water quality improving in storage reservoir by introducing of artificial phytolittoral.* Annual Set the Environment Protection, 20, 392-416.

Shen, Q., Wang, Y., Wang, X., Liu, X., Zhang, X. & Zhang, S. 2019. *Comparing interpolation methods to predict soil total phosphorus in the Mollisol area of Northeast China*. CATENA, 174, 59-72.

Shi, K., Zhang, Y., Zhu, G., Liu, X., Zhou, Y., Xu, H., Qin, B., Liu, G. & Li, Y., 2015. *Long-term remote monitoring of total suspended matter concentration in Lake Taihu using 250 m MODIS-Aqua data.* Remote Sensing of Environment, 164, 43-56.

Sojka, M., Jaskuła, J. & Wicher-Dysarz, J., 2016. *Assessment of biogenic compounds elution from the Glowna River catchment in the years 1996-2009.* Annual Set the Environment Protection, 18, 815-830.

Sojka, M., Jaskuła, J., Wicher-Dysarz, J. & Dysarz, T., 2017. *Analysis of selected reservoirs functioning in the Wielkopolska region.* Acta Scientiarum

Polonorum, Formatio Circumiectus, 16, 4, 205-215.

Soundharajan, B.S., Adeloye, A.J. & Remesan, R., 2016. *Evaluating the variability in surface water reservoir planning characteristics during climate change impacts assessment.* Journal of Hydrology, 538, 625-639.

Urbański, J.A., Wochna, A., Bubak, I., Grzybowski, W., Lukawska-Matuszewska, K., Łącka, M., Śliwińska S., Wojtasiewicz, B. & Zajączkowski, M., 2016. *Application of Landsat 8 imagery to regional-scale assessment of lake water quality*. International Journal of Applied Earth Observation and Geoinformation, 51, 28-36.

Vollenweider, R.A., 1976. *Advances in defining critical loading levels for phosphorus in lake eutrophication*. Mem. Ist. Ital. Idrobiol., 33, 53-83.

Wu, G., De Leeuw, J., Skidmore, A.K., Prins, H.H. & Liu, Y., 2008. *Comparison of MODIS and Landsat TM5 images for mapping tempo–spatial dynamics of Secchi disk depths in Poyang Lake National Nature Reserve, China*. International Journal of Remote Sensing, 29, 8, 2183-2198.

Xu, Y., Li, A.J., Qin, J., Li, Q., Ho, J.G. & Li, H., 2017. *Seasonal patterns of water quality and phytoplankton dynamics in surface waters in Guangzhou and Foshan, China.* Science of the Total Environment, 590, 361-369.

Yadav, S., Yoneda, M., Susaki, J., Tamura, M., Ishikawa, K. & Yamashiki Y., 2017. *A satellite-based assessment of the distribution and biomass of submerged aquatic vegetation in the optically shallow basin of Lake Biwa.* Remote Sensing, 9, 9, 966.

Yan, T., Bai, J., Arsenio, T., Liu, J. & Shen, Z., 2018. *Future climate change impacts on streamflow and nitrogen exports based on CMIP5 projection in the Miyun Reservoir Basin, China.* Ecohydrology & Hydrobiology, In Press.

Yüzügüllü, O. & Aksoy, A., 2011. *Determination of Secchi Disc depths in Lake Eymir using remotely sensed data.* Procedia-Social and Behavioral Sciences, 19, 586-592.

Zhang, W., Liu, P., Wang, H., Lei, X. & Feng, M., 2017. *Operating rules of irrigation reservoir under climate change and its application for the Dongwushi Reservoir in China*. Journal of Hydro-Environment Research, 16, 34-44.

Zhengjun, W., Jianming ,H. & Guisen, D., 2008. *Use of satellite imagery to assess the trophic state of Miyun Reservoir, Beijing, China.* Environmental Pollution, 155, 1, 13-19.

Zhou, Q., Zhang, Y., Li, K., Huang, L., Yang, F., Zhou, Y. & Chang, J., 2018. *Seasonal and spatial distributions of euphotic zone and long-term variations in water transparency in a clear oligotrophic Lake Fuxian, China*. Journal of Environmental Sciences, 72, 185-197.

Received at: 23. 12. 2018
Revised at: 25. 04 2019
Accepted for publication at: 05.05 2019
Published online at: 18. 05. 2019